The Journal of
Eukaryotic Microbiology

Published by the International Society of Protistologists

J. Eukaryot. Microbiol., 59(6), 2012 pp. 548–563

DOI: 10.1111/j.1550-7408.2012.00638.x

Morphological and Molecular Characterization of *Paramecium* (*Viridoparamecium* nov. subgen.) *chlorelligerum* Kahl 1935 (Ciliophora)

MARTIN KREUTZ,[a] THORSTEN STOECK[b] and WILHELM FOISSNER[c]

[a]*Private Laboratory, Am See 27, D-78465, Constance, Germany, and*
[b]*Department of Ecology, University of Kaiserslautern, Erwin-Schrödinger-Strasse 14, D-67663, Kaiserslautern, Germany, and*
[c]*Department of Organismic Biology, University of Salzburg, Hellbrunnerstrasse 34, A-5020, Salzburg, Austria*

ABSTRACT. We redescribe *Paramecium chlorelligerum*, a forgotten species, which Kahl (*Tierwelt Dtl.*, 1935, 30:651) briefly but precisely described in the addendum to his ciliate monographs as a *Paramecium* with symbiotic green algae. The redescription is based on classical morphological methods and the analysis of the small subunit (SSU) rDNA. Morphologically, *P. chlorelligerum* differs from *P.* (*C.*) *bursaria*, the second green species in the genus, by having a special swimming shape, the length of the caudal cilia, the size of the micronucleus, the size of the symbiotic algae, the contractile vacuoles (with collecting vesicles vs. collecting canals), and the number of excretory pores/contractile vacuole (1 vs. 2–3). The molecular investigations show that *P. chlorelligerum* forms a distinct branch distant from the *P.* (*Chloroparamecium*) *bursaria* clade. Thus, we classify *P. chlorelligerum* in a new subgenus: *Paramecium* (*Viridoparamecium*) *chlorelligerum*. The symbiotic alga belongs to the little-known genus *Meyerella*, as yet recorded only from the plankton of a North American lake.

Key Words. Biodiversity, *Chloroparamecium*, Germany, *Meyerella*, Oligohymenophora, Simmelried moorland.

THERE is a world of cell biological, ultrastructural, genetic, and ecological studies on *Paramecium* spp. (for reviews, see Görtz 1988; Kahl 1931; Plattner 2002; Plattner and Kissmehl 2003; Przyboś and Fokin 2000; Przyboś et al. 2006; Wichterman 1986), while morphological taxonomy of species has been badly neglected (e.g. we are still waiting for a fundamental revision of the genus). More important recent genetic and morphological studies are those from Sonneborn (1975), Dragesco and Dragesco-Kernéis (1986), and especially, those from Fokin's laboratory in St. Petersburg (Fokin 1986, 1997, 2010/11; Fokin and Chivilev 1999; Fokin et al. 1999a, b, 2004, 2005). The research of the Russian group and molecular investigations by others (Hoshina et al. 2006; Strüder-Kypke et al. 2000) not only contributed to the general knowledge of the genus but also supported the early subgeneric split of the genus by Jankowski (1972).

Recent molecular studies on the symbionts of the supposed single green species of the genus *Paramecium*, i.e. on *P.* (*Chloroparamecium*) *bursaria* showed that this species has acquired various genera of green algal symbionts several times independently (for reviews, see Hoshina and Imamura 2008; Nakahara et al. 2004).

While higher classifications often come and go, a well-described species lasts forever. Here, we redescribe such a species, *P. chlorelligerum*, which Kahl (1935) briefly but precisely described in the addendum to his ciliate monographs as a *Paramecium* with symbiotic green algae. Revisers, however, have neglected it or declared *P. chlorelligerum* as "an unacceptable and therefore suppressed species" (Wichterman 1986). We shall show that *P. chlorelligerum* is not only a distinct morphospecies but also belongs to a molecular clade distant from *P.* (*C.*) *bursaria*, showing that green algal symbiosis was acquired in at least two *Paramecium* clades.

MATERIALS AND METHODS

Material. *Paramecium* (*Viridoparamecium*) *chlorelligerum* was rediscovered in the Simmelried moorland, a protist diversity hotspot studied by Kreutz and Foissner (2006). Briefly, it is a very small, only three-hectare-sized *Sphagnum* wetland in southern Germany near the town of Constance (GPS location: 47°43.05′N/9°05.61′E). In October 2010, *P.* (*V.*) *chlorelligerum* occurred in *Sphagnum* pond II and the mire outlet, where it sometimes reached abundances of up to ~ 200 cells/ml. However, often they colonized areas of only about 0.5 m^2 in size, where the decaying leaf litter was overgrown and held together by *Beggiatoa alba* (Fig. 1, 2). The water temperature was 8 °C and pH was 5.7. The brownish water was clear and had a mouldy smell; H_2S smell occurred when the leaf layer was disturbed. The leaf layer was colonized not only by *Beggiatoa* but also by a great variety of autotrophic and heterotrophic protists and micro-metazoans, many of which are typical indicators of microaerobity or anaerobity (e.g. *Pseudoblepharisma tenue*, *Loxodes striatus*, *Euplotes daidaleos*, *Frontonia viridis*, and *Metopus striatus*). *Paramecium* (*V.*) *chlorelligerum* was especially abundant in minute, green accumulations of algae and was found again in autumn 2011 (Fig. 2). Various culture attempts failed and very few dividers and conjugants were seen in the sampling jars, where the number of cells strongly decreased within a week. Thus, all investigations were performed on environmental material.

Paramecium (*Chloroparamecium*) *bursaria* occurred together with *P.* (*V.*) *chlorelligerum* but was much less abundant.

Paramecium (*Cypriostomum*) *nephridiatum* was collected from the mud of a stream in the surroundings of the town of Gunzenhausen, Bavaria, Germany (49°20′N/10°45′E). Pure, nonclonal cultures were set up with tap water containing some squashed wheat grains.

Morphological methods. Field material as described above was used for all investigations. Living cells were studied using a high-power oil immersion objective and differential interference contrast. Live micrographs were shot with flash. Preparations were performed as described by Foissner (1991, 2003). However, silver carbonate and protargol preparations were difficult due to the symbiotic algae. The oral structures were revealed with the protargol method of Wilbert (1975). Counts and measurements on silvered specimens were conducted at a magnification of 1,000X. In vivo measurements were based on light micrographs and were performed at magnifications of 100–1,000X. Illustrations of live specimens were based on micrographs, while those of prepared cells were made with a drawing device.

Molecular analyses. To extract genomic DNA for the 18S rRNA phylogenies of *P.* (*V.*) *chlorelligerum* and its symbiont, about 20 *Paramecium* specimens were picked with a micropipette and transferred into 180 µl Tissue lysis buffer (Qiagen, Hildesheim, Germany) and 20 µl Proteinase K (20 mg/ml).

Corresponding Author: W. Foissner, FB Organismische Biologie, Universität Salzburg, Hellbrunnerstrasse 34, A-5020 Salzburg, Austria—Telephone number: +43 0 662 8044 5615; FAX number: +43 0 662 8044 5698; e-mail: wilhelm.foissner@sbg.ac.at

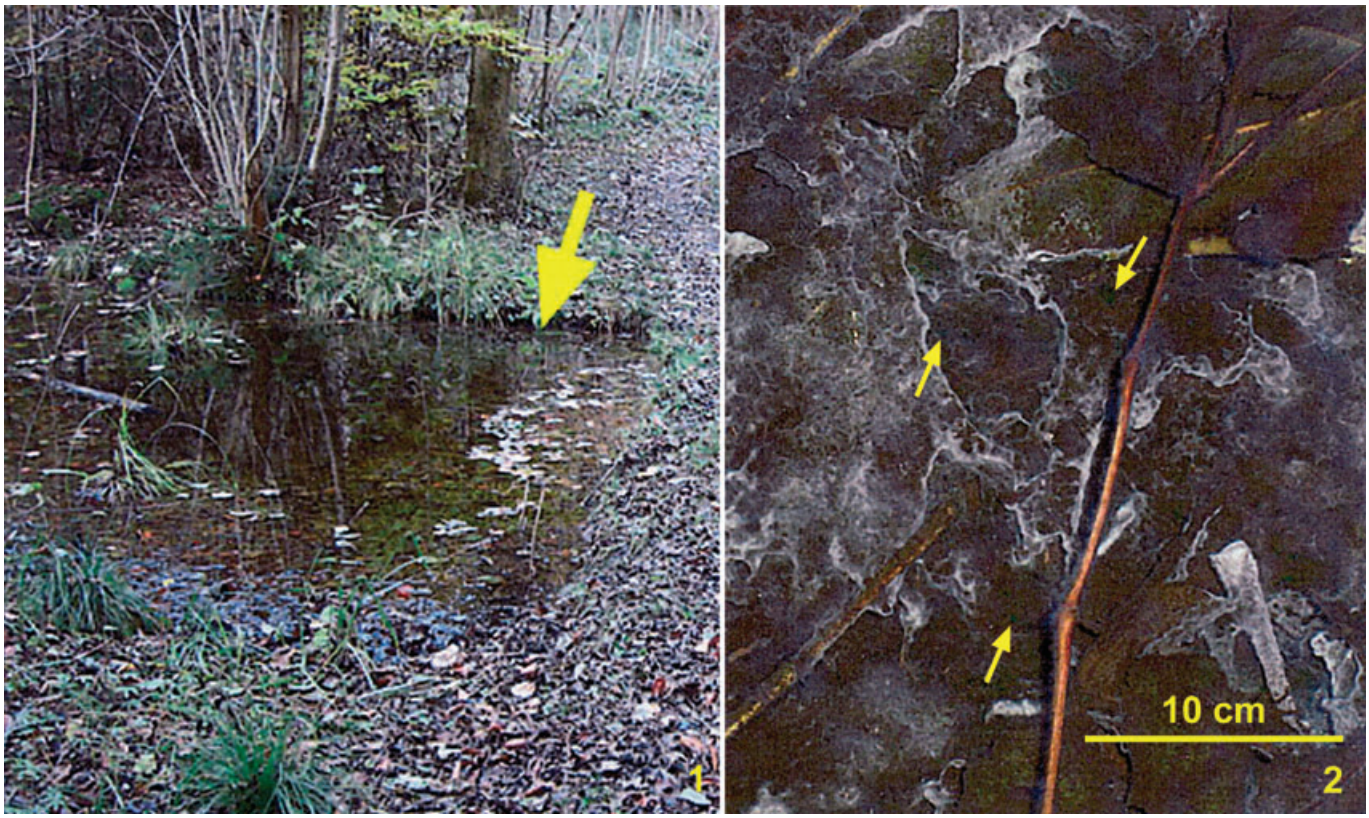

Fig. **1**–2. Photographs from the mire outlet, where *Paramecium* (*Viridoparamecium*) *chlorelligerum* was rediscovered in October 2010. **1.** A puddle within the outlet. The arrow marks the region shown in Fig. 2 at higher magnification. **2.** Bottom of the puddle shown in Fig. 1. The leaf litter is bound and partially overgrown by the whitish sulphur bacterium *Beggiatoa alba* and a great variety of autotrophic and heterotrophic protists and micro-metazoa. The arrows mark minute, green accumulations of *P.* (*V.*) *chlorelligerum* and green algae.

Subsequently, the genomic DNA was extracted using the protocol for cultured animal cells of the DNEasy Tissue Kit (Qiagen). The 18S rRNA genes were amplified using the universal eukaryotic primers 82F and 1492R SEQS (Lopez-Garcia et al. 2001; Medlin et al. 1988). The amplification reaction contained 10–20 ng of DNA template, 2.5 U HotStar Taq DNA polymerase (Qiagen) in the manufacturer-provided reaction buffer, 1.5 mM $MgCl_2$, 200 µM of each dNTP, and 0.5 µM of each oligonucleotide primer. The final volume was adjusted to 50 µl with sterile distilled water. The PCR protocol for 18S rDNA gene amplification consisted of an initial hot start incubation of 15 min at 95 °C followed by 30 identical amplification cycles (i.e. denaturing at 95 °C for 45 s, annealing at 55 ° C for 1 min, and extension at 72 °C for 2.5 min), and a final extension at 72 °C for 7 min. Negative control reactions included *Escherichia coli* DNA as a template. The resulting PCR products were cleaned with the PCR MinElute Kit (Qiagen) and cloned into a vector, using the TA-Cloning kit (Invitrogen, Carlsbad, CA). Plasmids were isolated with Qiaprep Spin Miniprep Kit (Qiagen) from overnight, PCR-reamplified cultures, using M13F and M13R primers to screen for inserts of the expected size (~ 1.5 kb). Fragments with the expected length were digested with the restriction enzyme Hae III (New England Biolabs), according to the manufacturer's protocol, to distinguish host and symbiont genes.

Clones with different restriction patterns were sequenced bidirectionally using M13 sequence primers with the Big Dye terminator kit (Applied Biosystems, Foster City, CA) on an ABI 3730 automated sequencer.

For assessment of the phylogenetic placement of *P.* (*V.*) *chlorelligerum,* its 18S rDNA sequence was aligned to 18S rDNA sequences of other *Paramecium* species available in GenBank. The symbiont sequence was aligned to its closest GenBank BLASTn hits and selected representative Trebouxiophyceae. Alignments were constructed using Muscle (Edgar 2004) and were refined using Gblocks (Castresana 2000), followed by eye inspection and manual refinement. The resulting alignments included 1,763 characters and 31 taxa for *Paramecium* and 1,701 characters from 27 taxa of the Trebouxiophyceae. Both alignments are available from the authors on request. Evolutionary distance and maximum-likelihood (ML) analyses were conducted for phylogenies. Neighbour-joining evolutionary distances (BioNJ) were carried out in the Seaview program package (vers. 4.2, Galtier et al. 1996). Maximum-likelihood bootstrap analyses were carried out with 1,000 replicates, using RAxML with the setting as described in Stamatakis et al. (2008). ML analyses were conducted online on the CIPRES Portal V 2.0 (http://www.phylo.org.). Pairwise sequence similarities were calculated with the module pairalign as implemented in the JAguc software package (http://wwwagak.informatik.uni-kl.de/JAguc). The GenBank accession numbers of *P.* (*V.*) *chlorelligerum* and its symbiont are JX010740 and JX010741, respectively.

Table **1.** Morphometric data on *Paramecium (Viridoparamecium) chlorelligerum* (PC) and *Paramecium (Chloroparamecium) bursaria* (PB).

Characteristics[a]	Species	Method	$\bar{x}$	M	SD	SE	CV	Min	Max	*n*
Body, length (μm)	PC	IV	115.8	117.0	9.0	1.8	7.8	101.0	140.0	25
	PB	IV	139.3	140.0	11.7	2.6	8.4	110.0	158.0	21
	PC	CHL	111.8	112.0	3.8	0.8	3.4	106.0	120.0	21
	PB	CHL	113.2	110.0	8.7	2.8	7.7	101.0	129.0	10
	PC	SEM	102.0	102.0	10.0	2.5	9.8	80.0	116.0	16
Body, width (μm)	PC	IV	48.5	47.0	6.7	1.3	13.9	37.0	61.0	25
	PB	IV	60.2	61.0	7.2	1.6	11.9	48.0	71.0	21
	PC	CHL	51.2	51.0	4.9	1.1	9.5	41.0	60.0	21
	PB	CHL	49.2	49.5	5.1	1.6	10.4	40.0	56.0	10
	PC	SEM	49.9	50.5	4.8	1.2	9.6	41.2.	59.4	16
Body, length: width, ratio	PC	IV	2.4	2.4	0.2	0.0	8.8	2.1	2.9	25
	PB	IV	2.3	2.3	0.3	0.1	11.4	1.9	3.0	21
	PC	CHL	2.2	2.2	0.2	0.0	7.8	1.9	2.6	21
	PB	CHL	2.3	2.3	0.2	0.1	10.1	2.0	2.8	10
	PC	SEM	2.0	2.0	0.2	0.1	7.8	1.9	2.4	16
Anterior body end to anterior margin of mouth entrance, distance (μm)	PC	CHL	51.3	52.0	2.7	0.6	5.3	47.0	57.0	21
	PB	CHL	45.4	46.0	5.6	1.8	12.3	37.0	54.0	10
Posterior margin of mouth entrance to posterior end of cell, distance (μm)	PC	CHL	48.0	47.0	3.5	0.8	7.4	43.0	56.0	21
	PB	CHL	47.0	46.0	4.9	1.6	10.4	40.0	53.0	9
Mouth entrance, length (μm)	PC	CHL	13.1	13.0	1.0	0.2	8.0	12.0	15.0	21
	PB	CHL	14.5	14.0	1.4	0.5	9.9	13.0	18.0	10
Mouth entrance, width (μm)	PC	CHL	4.5	4.0	0.9	0.2	20.7	3.0	6.0	21
	PB	CHL	5.7	5.0	1.1	0.4	19.5	5.0	8.0	7
Anterior body end to first excretory pore, distance (μm)	PC	CHL	34.2	34.0	5.2	1.1	15.1	26.0	42.0	21
	PB	CHL	36.8	38.5	6.0	1.9	16.2	28.0	44.0	10
Excretory pores, number for anterior vacuole	PC	CHL	1.0	1.0	0.0	0.0	0.0	1.0	1.0	21
	PB	CHL	2.0	2.0	0.0	0.0	0.0	2.0	2.0	10
Excretory pores, distance between anterior and posterior pores (μm)	PC	CHL	49.9	49.0	5.0	1.1	10.0	40.0	60.0	21
	PB	CHL	40.4	39.0	6.2	2.1	15.3	33.0	51.9	9
Posterior body end to first excretory pore, distance (μm)	PC	CHL	26.0	26.0	2.0	0.4	7.9	22.0	29.0	21
	PB	CHL	28.4	29.5	3.7	1.2	12.9	23.0	33.0	10
Excretory pores, number for posterior vacuole	PC	CHL	1.0	1.0	0.0	0.0	0.0	1.0	1.0	21
	PB	CHL	2.0	2.0	0.5	0.1	23.6	1.0	3.0	10
Anterior body end to begin of cytopyge silverline, distance (μm)	PC	CHL	86.6	87.0	3.4	0.7	3.9	79.0	91.0	21
	PB	CHL	88.8	89.0	8.9	3.2	10.1	76.0	105.0	8
Anterior body end to macronucleus, distance (μm)	PC	CHL	45.0	45.0	10.1	2.2	22.4	26.0	65.0	21
	PB	CHL	40.1	40.0	5.3	1.7	13.1	32.0	50.0	10
Macronucleus, length (μm)	PC	CHL	20.3	20.0	2.7	0.6	13.0	16.0	27.0	21
	PB	CHL	25.2	25.5	2.7	0.9	10.9	20.0	29.0	10
Macronucleus, width (μm)	PC	CHL	13.7	14.0	1.6	0.4	11.8	10.0	17.0	21
	PB	CHL	11.7	11.0	2.1	0.7	18.0	10.0	16.0	10
Micronucleus, length (μm)	PC	IV	5.7	5.7	0.7	0.2	12.6	4.1	6.9	19
	PB	IV	14.7	14.0	1.7	0.5	11.8	12.0	18.0	11
Micronucleus, width (μm)	PC	IV	2.4	2.4	0.3	0.1	12.8	1.9	2.9	19
	PB	IV	6.6	7.0	0.9	0.3	13.9	5.0	8.0	11
Symbiotic algae, length (μm)	PC	IV	7.7	7.7	1.3	0.3	16.5	4.8	9.6	21
	PB	IV	5.5	5.7	0.7	0.2	12.8	4.3	6.7	21
Symbiotic algae, width (μm)	PC	IV	6.2	6.3	1.4	0.3	22.4	3.4	9.6	21
	PB	IV	5.1	5.1	0.7	0.2	13.7	3.5	6.0	21
Symbiotic algae, number/cell[a]	PC	IV	519.5	498.0	141.1	35.3	27.2	287.0	809.0	16
	PB	IV	594.0	590.0	190.5	43.7	32.1	287.0	951.0	19
Ciliary rows, number in mid-body in 20 μm of dorsal side	PC	CHL	12.2	12.0	1.5	0.3	12.1	9.0	14.0	21
	PB	CHL	15.2	14.0	2.7	0.9	18.0	12.0	20.0	10
Caudal cilia, length (μm)	PC	IV	29.0	29.0	4.5	0.9	15.5	21.0	40.0	23
	PB	IV	18.4	18.5	1.8	0.4	10.0	13.0	21.0	20
Oral polykinetid 1, length (μm)	PC	P	11.6	12.0	1.5	0.4	13.0	8.0	14.0	15
Oral polykinetid 2, length (μm)	PC	P	18.7	18.0	1.3	0.3	6.9	17.0	22.0	15
Oral polykinetid 3, length (μm)[b]	PC	P	24.4	25.0	1.5	0.4	6.2	21.0	28.0	15

Data based on randomly selected environmental specimens.

[a]Counted from squashed, photographed specimens.

[b]This polykinetid is distinctly sigmoidal. Only the longitudinal axis of the "S" has been measured.

CHL = Chatton–Lwoff silver nitrate impregnation; CV = coefficient of variation in %; IV = in vivo and freely motile; M = median; Max = maximum; Min = minimum; *n* = number of specimens investigated; P = protargol impregnation; SD = standard deviation; SE = standard error of mean; SEM = scanning electron microscopy; $\bar{x}$ = arithmetic mean.

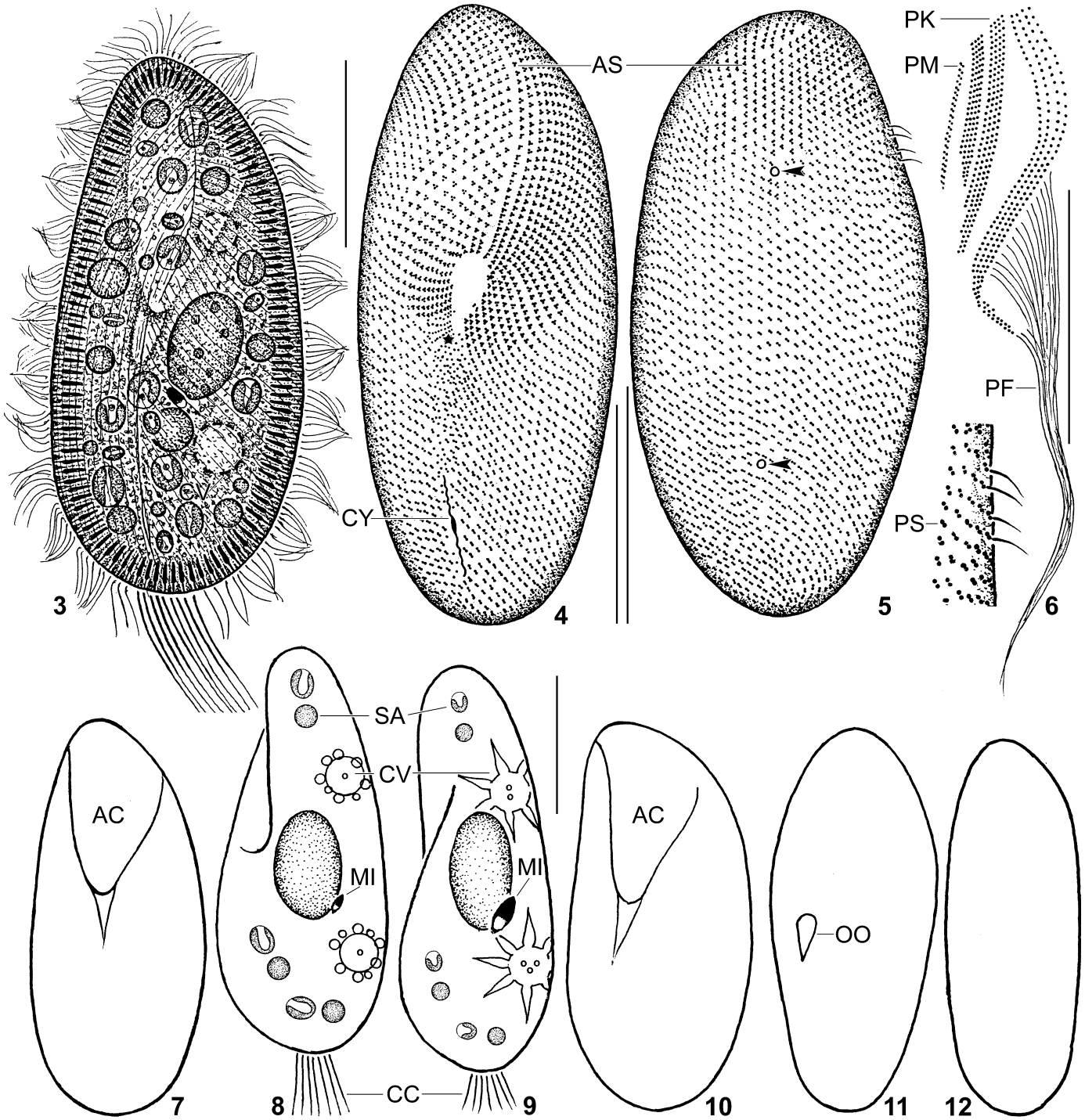

Fig. **3–12.** *Paramecium* (*Viridoparamecium*) *chlorelligerum* (3–8, 11, 12) and *Paramecium* (*Chloroparamecium*) *bursaria* (9, 10) from life (3, 7–12), after Chatton–Lwoff silver nitrate impregnation (4, 5), and after protargol impregnation (6). **3.** Ventral view of a representative specimen, length 115 μm. Note the long caudal cilia and the symbiotic algae, of which only some are shown. **4, 5.** Ventral and dorsal view of kinetid (ciliary) pattern of main voucher specimens, length 112 μm and 102 μm. The asterisk denotes a postoral patch of nonciliated basal bodies (cp. Fig. 58). The arrowheads mark the excretory pores of the contractile vacuoles. **6.** The oral ciliature consists of a short paroral membrane and three polykineties, of which the leftmost, called quadrulus, is the longest and consists of four comparatively widely spaced ciliary rows. The individual ciliary rows of the polykinetids end proximally at various, fairly constant levels. **7, 10.** Ventral view of *P.* (*V.*) *chlorelligerum* and *P.* (*C.*) *bursaria*, which are indistinguishable in body size and shape. **8, 9.** Lateral view of *P.* (*V.*) *chlorelligerum* and *P.* (*C.*) *bursaria*, showing the main morphological differences: the length of the caudal cilia, the size of the micronucleus and symbiotic algae, and the structure of the contractile vacuoles (with collecting vesicles and one pore vs. with collecting canals and two to three pores). **11, 12.** When *P.* (*V.*) *chlorelligerum* is disturbed, it becomes a rapidly swimming ellipsoidal ciliate not recognizable as a *Paramecium*. AC, preoral concavity; AS, anterior (preoral) suture; CC, caudal cilia; CV, contractile vacuoles; CY, cytopyge in postoral suture; MI, micronuclei; OO, oral opening; PF, pharyngeal fibres; PM, paroral membrane; PS, parasomal sac; SA, symbiotic algae. Scale bars 20 μm (Fig. 6) and 40 μm (Fig. 3–5, 7–12).

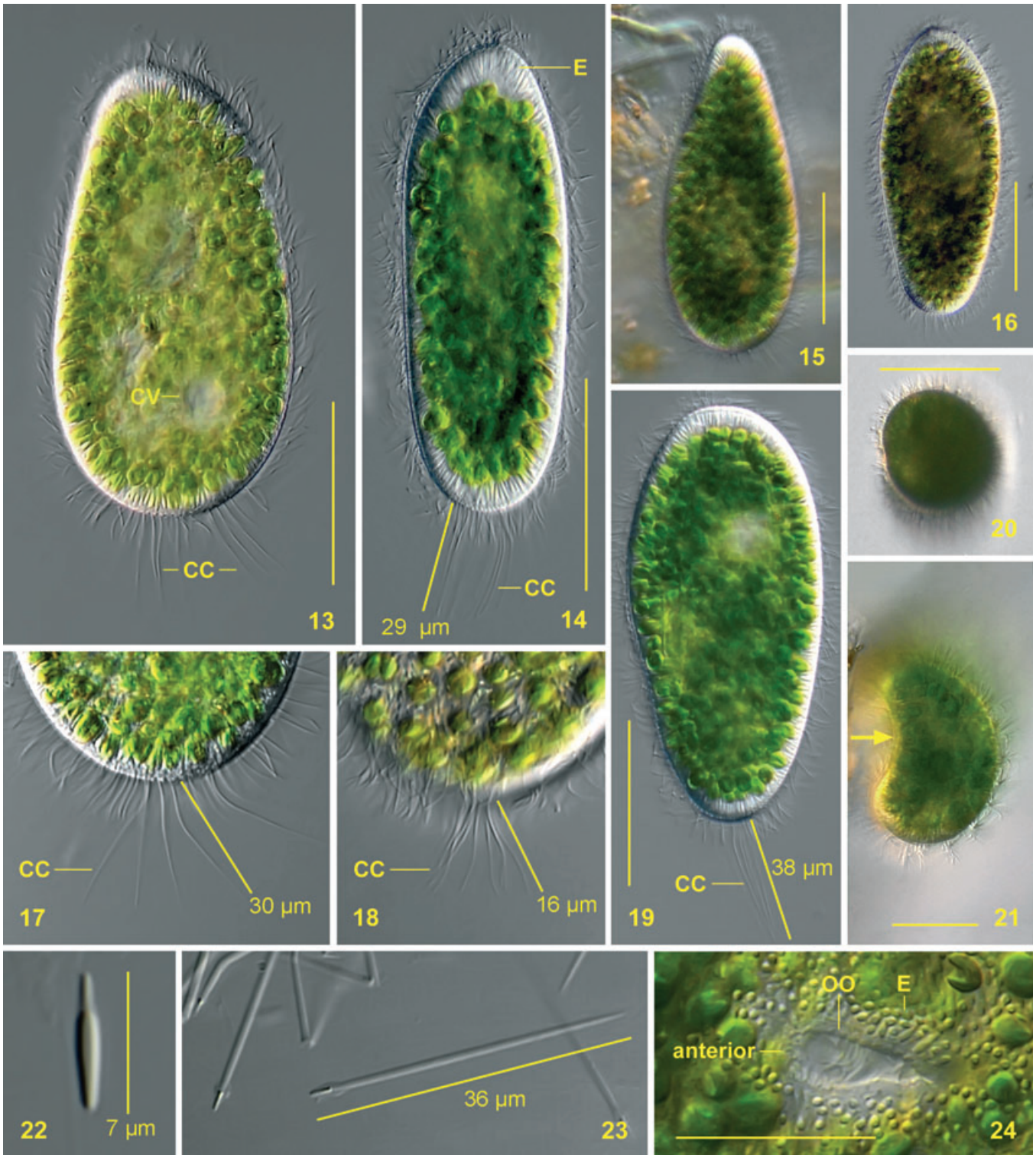

Fig. **13–24.** *Paramecium* (*Viridoparamecium*) *chlorelligerum* (13–17, 19–24) and *Paramecium* (*Chloroparamecium*) *bursaria* (18) from life, using flash photomicrography of freely motile specimens, except of Fig. 22, 23. **13.** Ventral view focused to dorsal side. The body size and shape of resting specimens of *P.* (*V.*) *chlorelligerum* and *P.* (*C.*) *bursaria* (Fig. 27) are so similar that they cannot be distinguished with these features. **14, 16, 19.** When *P.* (*V.*) *chlorelligerum* is disturbed, the shape becomes ellipsoidal to cylindroidal and the movement becomes very rapid. In this state, it is hardly recognizable as a *Paramecium*. **15.** A rapidly swimming specimen attaching to organic debris and assuming the broad resting state. **17, 18.** The caudal cilia of *P.* (*V.*) *chlorelligerum* are nearly twice as long as those of *P.* (*C.*) *bursaria*. **20.** Transverse view of a rapidly swimming cell. **21.** Transverse view in anterior body half, showing the preoral concavity (arrow). **22, 23.** Resting and exploded trichocysts. **24.** Oral opening. CC, caudal cilia; CV, contractile vacuole; E, extrusomes; OO, oral opening. Scale bars 20 µm (Fig. 21, 24), 40 µm (Fig. 20), and 50 µm (13–16, 19).

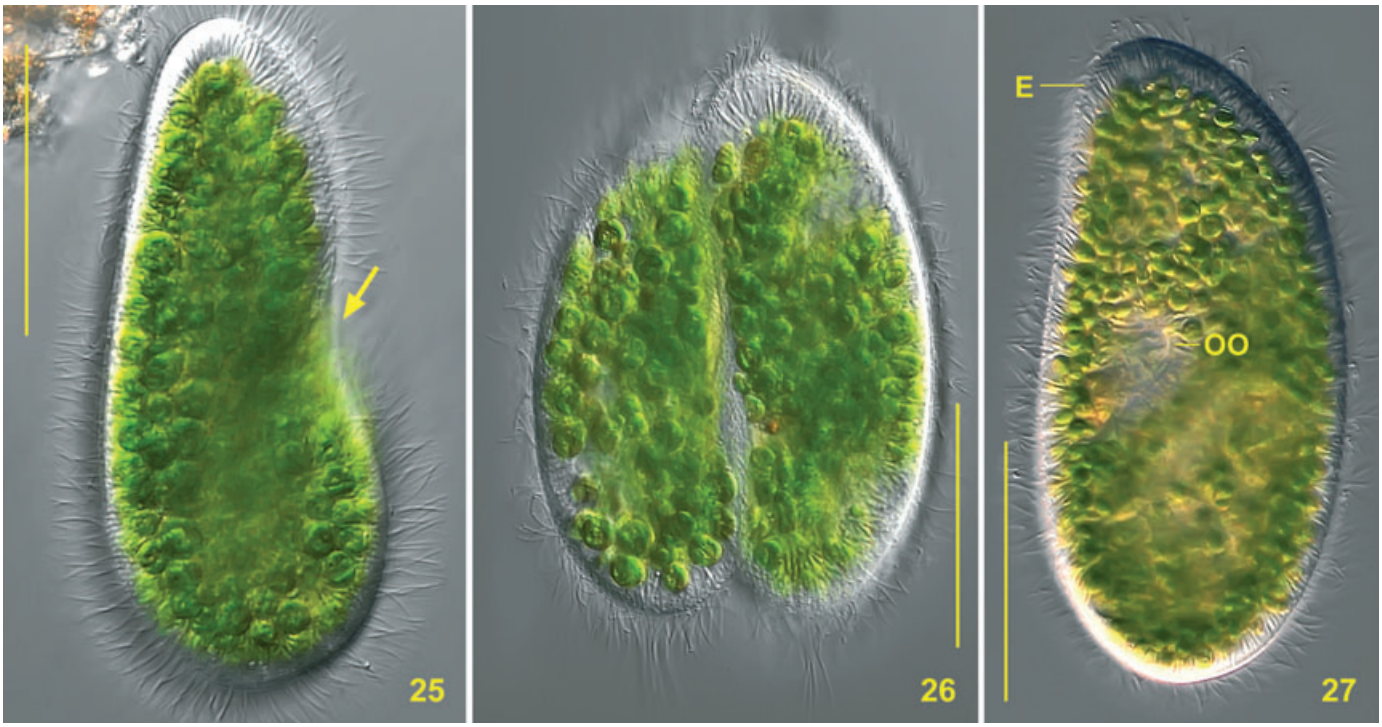

Fig. **25–27.** *Paramecium* (*Viridoparamecium*) *chlorelligerum* (25, 26) and *Paramecium* (*Chloroparamecium*) *bursaria* (27) from life, using flash photomicrography of freely motile specimens. **25.** A rapidly swimming specimen turning to the broad resting state (Fig. 13). Arrow marks mouth area. **26.** A conjugation pair was observed in a fresh sample in autumn 2011. **27.** Ventral view. The body size and shape of *P.* (*C.*) *bursaria* and resting specimens of *P.* (*V.*) *chlorelligerum* (Fig. 13) are so similar that they cannot be distinguished with these features.

RESULTS

Redescription of *Paramecium* (*Viridoparamecium*) *chlorelligerum* (Table 1 and Fig. 3–8, 11–17, 19–26, 28–33, 40, 41, 44, 46, 50–60, 62–64). **Body size.** The size of *P.* (*V.*) *chlorelligerum* showed little variability, both in vivo and in silver nitrate preparations (i.e. length CV 7.8 and 3.4%, Table 1). The average size of live specimens was 116 × 48 μm; thus, the cells are ellipsoidal (~ 2:1) to elongate ellipsoidal (> 2:1). The preparation shrinkage was low: only 3.5% due to the osmium fixation. In the scanning electron microscopic (SEM) preparations, the length shrinkage was 12% but the width increased by 3% (Table 1).

Body shape and movement. *Paramecium* (*V.*) *chlorelligerum* has a "resting shape" and a "swimming shape". The two shapes are so different that they appear to belong to different species (Fig. 3, 11, 12–14, 16, 19). Although using video microscopy (video clip in Video S1), we could not clarify how the shape changes are achieved. However, one can recognize that the preoral concavity disappears.

When undisturbed, the cells stay almost motionless on the microscope slide, performing short, jerky movements. The resting shape is assumed when the cell is slowly gliding or swimming or is motionless for some time collecting food particles. The resting cells are ellipsoidal to elongate ellipsoidal with a more or less distinct oblique truncation of the left lateral preoral region. Thus, the posterior half is usually slightly wider than the anterior one (Fig. 3, 7, 13). The cells are flattened dorsoventrally, especially preorally, where the central region of the ventral side is concave and extends to the mouth opening (Fig. 3, 7, 13, 21). The preoral concavity disappears both in silver nitrate and SEM preparations (Fig. 46, 50, 51, 54).

If *P.* (*V.*) *chlorelligerum* is disturbed, for instance, by mixing the drop with a needle, the behaviour and body shape change dramatically within a few seconds: the cells now swim very rapidly rotating counterclockwise about the main body axis; the preoral concavity disappears, making the cell body circular in transverse view (Fig. 20); and the body narrows, becoming elongate ellipsoidal (Fig. 11, 12, 14, 16, 19). When disturbance ends, the cells gradually slow down and assume the resting shape within about 30 s (Fig. 15, 25 and a video clip in Video S1).

Nuclear apparatus. The nuclei are slightly posterior of midbody in the left half of the cell (Table 1 and Fig. 3). The macronucleus is broadly to ordinarily ellipsoidal, i.e. on average 20 × 14 μm in silver nitrate-prepared specimens (Table 1). It has a distinct membrane and contains indistinct accumulations of argyrophilic material (Fig. 3, 40, 41). A single micronucleus with an average in vivo size of 5.7 × 2.4 μm is attached to the macronucleus (Table 1). The micronucleus belongs to the "compact" type (Fokin 1997): it has a deeply impregnating compact region and a hyaline "achromatic cap" (Fig. 3, 8, 40, 41).

Contractile vacuoles and cytopyge. There are two contractile vacuoles: the anterior vacuole is on average 34 μm distant from the body end, whereas the posterior one is 26 μm off the body end (Table 1 and Fig. 3, 5, 8, 13, 28–33, 53). The contractile vacuoles are surrounded by small collecting vesicles during the diastole (Fig. 30). Invariably, each vacuole has a single excretory pore. The cytopyge is as typical for *Paramecium*: it is in the postoral suture and its silverline extends in the posterior fifth of the cell (Table 1 and Fig. 4, 46, 50–52).

Cortex and extrusomes. *Paramecium* (*V.*) *chlorelligerum* has a typical *Paramecium* cortex with quadrangular and hexagonal kinetosome territories (Fig. 56, 59). Likewise, the extrusomes are typical, being composed of a very narrowly obovate shaft and a conical tip attached to the cortex. When resting, the

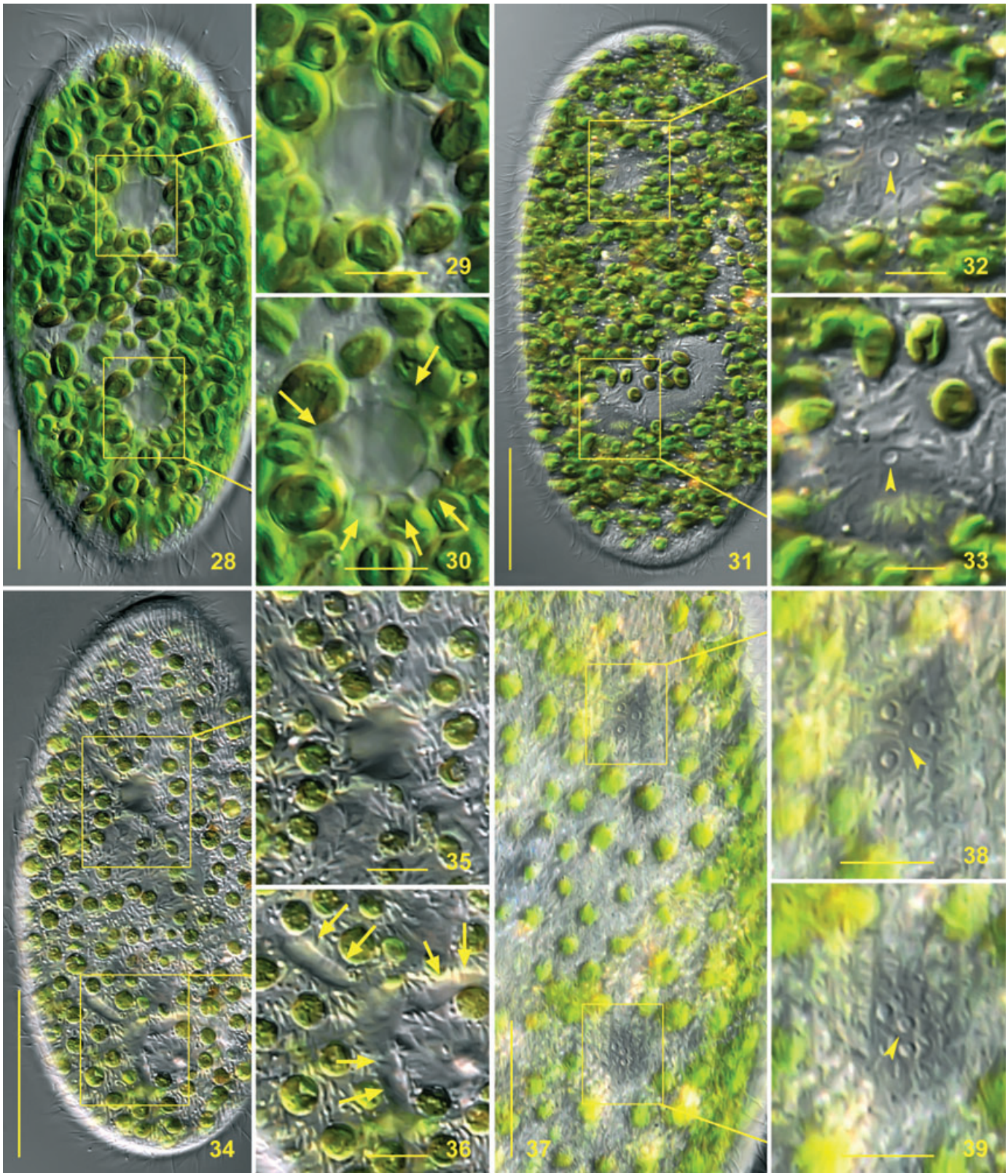

Fig. **28–39.** Slightly squeezed living specimens, showing the structure of the contractile vacuoles in *Paramecium* (*Viridoparamecium*) *chlorelligerum* (28–33) and *Paramecium* (*Chloroparamecium*) *bursaria* (34–39). The contractile vacuoles of *P.* (*V.*) *chlorelligerum* have collecting vesicles (28–30, arrows) and an excretory pore each (31–33, arrowheads) while those of *P.* (*C.*) *bursaria* have collecting canals (34–36, arrows) and two to three excretory pores each (37–39, arrowheads). Scale bars 10 μm (Fig. 29, 30, 32, 33, 35, 36, 38, 39) and 30 μm (Fig. 28, 31, 34, 37). Taken using flash photomicrography.

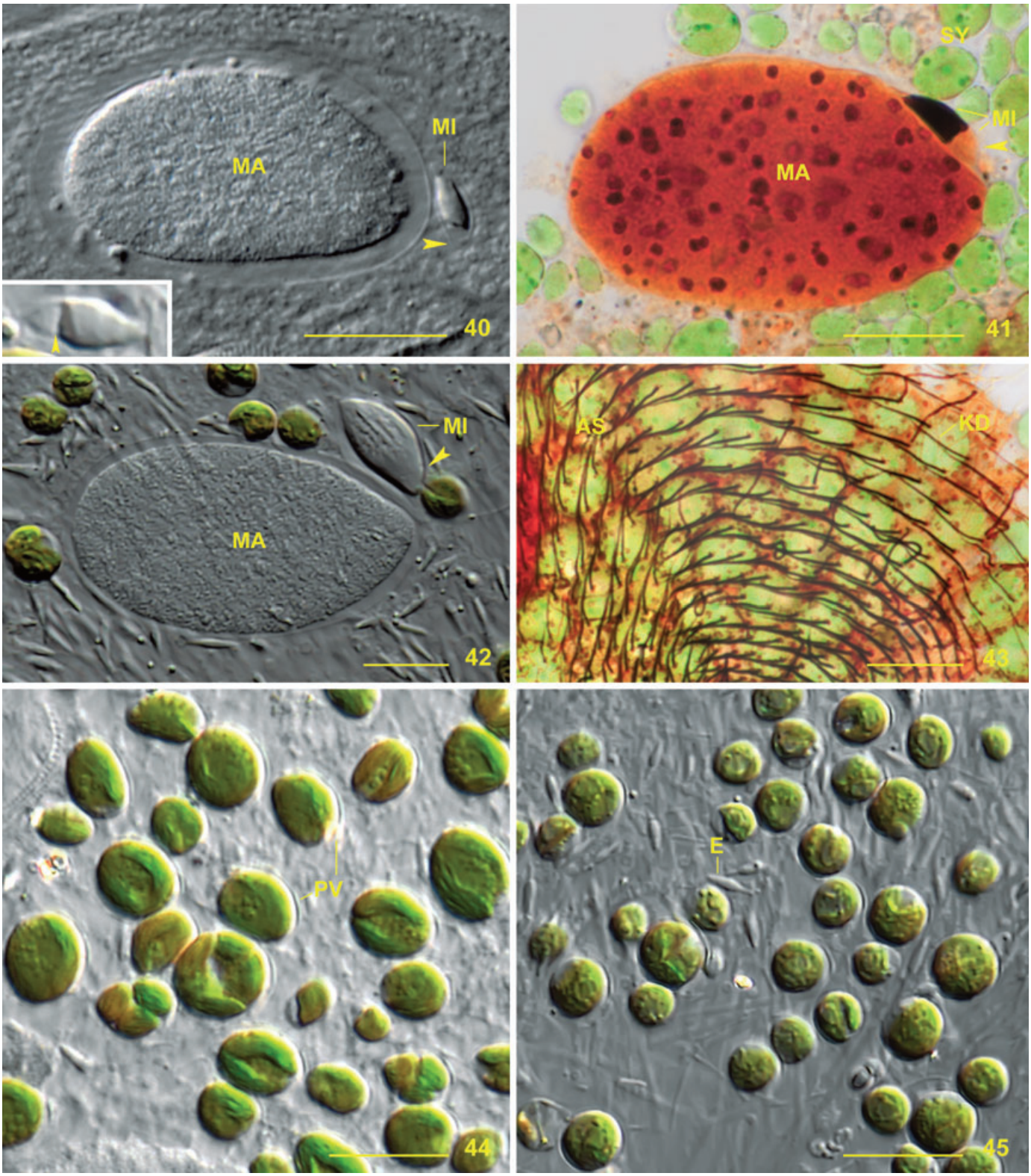

Fig. **40–45.** *Paramecium* (*Viridoparamecium*) *chlorelligerum* (40, 41, 43, 44) and *Paramecium* (*Chloroparamecium*) *bursaria* (42, 45) from life (40, 42, 44, 45) and after silver carbonate impregnation (41, 43). **40–42.** Both species have a single, compact type of micronucleus (Fokin 1997) but that of *P.* (*C.*) *bursaria* (Fig. 42) is about thrice as large as that of *P.* (*V.*) *chlorelligerum* (Table 3 and Fig. 40, 41). The arrowheads mark the hyaline "achromatic cap" which contains microtubule-like structures (Fokin 1997). **43.** Preoral region, showing the anterior suture and the long kinetodesmal fibres attaching to the basal bodies. **44, 45.** The symbiotic algae are considerably larger and more ellipsoidal ($\bar{x}$ 7.7 × 6.2 μm) in *P.* (*V.*) *chlorelligerum* (Fig. 44) than in *P.* (*C.*) *bursaria* ($\bar{x}$ 5.5 × 5.1 μm). AS, anterior suture; E, extrusome; KD, kinetodesmal fibre; MI, micronucleus; MA, macronucleus; PV, membrane of the perialgal vacuole; SY, symbiotic algae. Scale bars 10 μm.

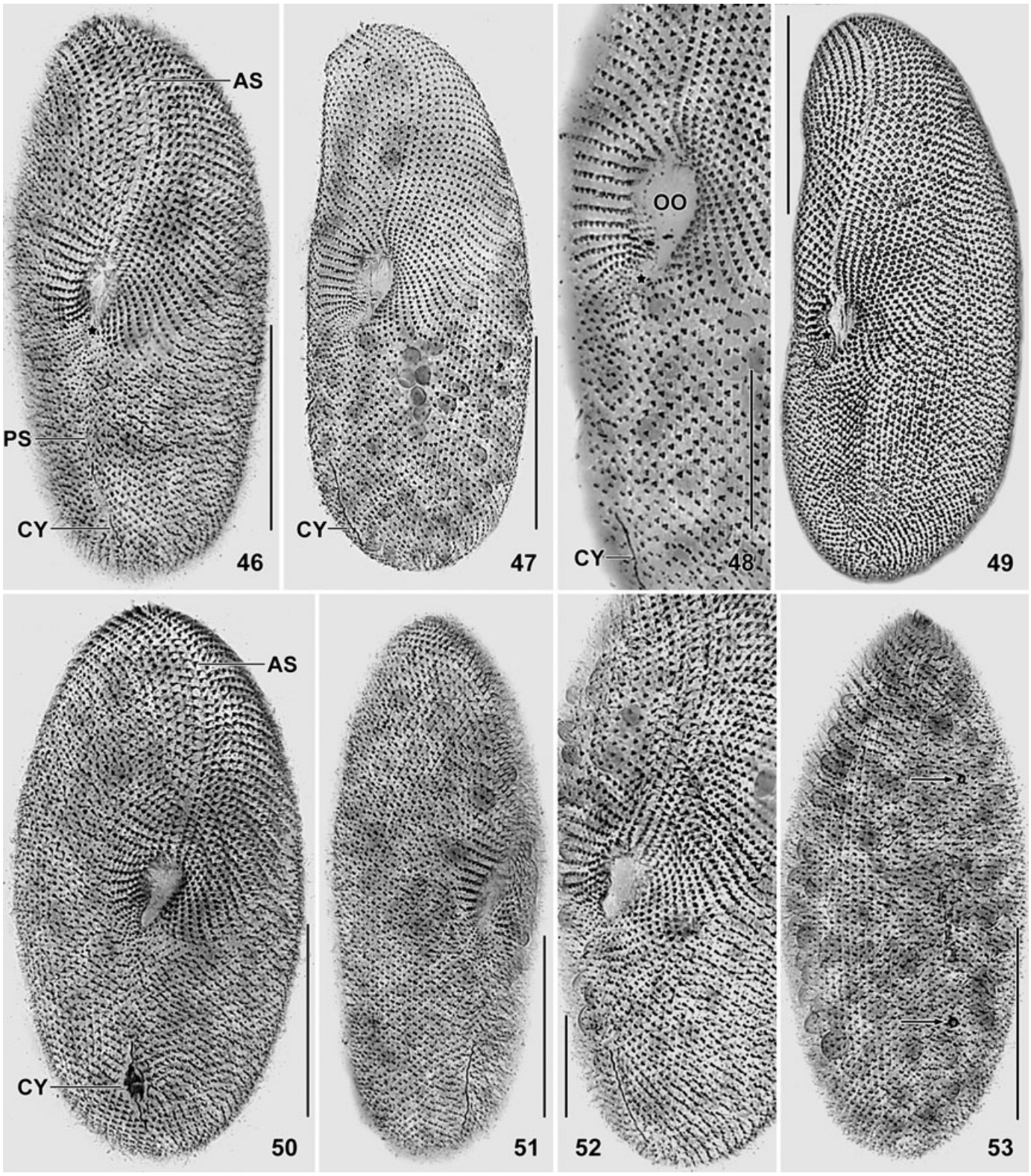

Fig. **46–53.** *Paramecium* (*Viridoparamecium*) *chlorelligerum* (46, 50–53), *P.* (*Chloroparamecium*) *bursaria* (47, 48), and *Paramecium* (*Cyrtostomum*) *nephridiatum* (49) after Chatton–Lwoff silver nitrate impregnation, showing various cortical structures. **46–49.** Ventral views, showing a postoral field of nonciliated monokinetids (asterisks). A comparison of the ciliary pattern shows that it is too similar for separating the three species. However, the oral opening is in mid-body in *P.* (*V.*) *chlorelligerum* (46) and *P.* (*V.*) *bursaria* (47) while posterior of mid-body in *P.* (*C.*) *nephridiatum*, which matches the data of Fokin et al. (1999b). **50.** Ventral view of an ellipsoidal specimen. **51, 52.** Right and left side view. **53.** Dorsal view, showing the excretory pores of the contractile vacuoles (arrows). AS, anterior suture; CY, cytopyge; OO, oral opening; PS, postoral suture. Scale bars 20 μm (Fig. 48, 52) and 40 μm (Fig. 46, 47, 49–51, 53).

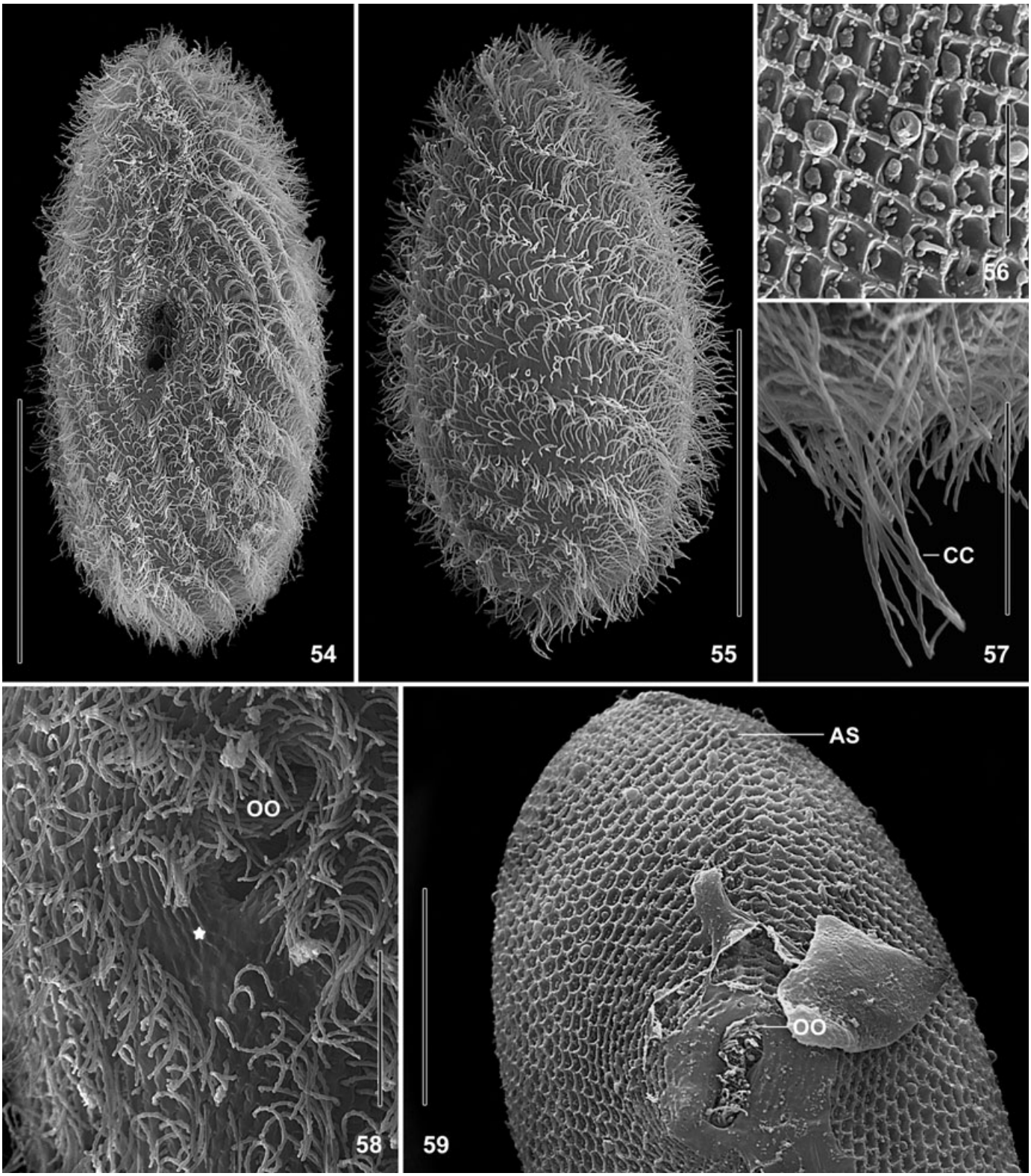

Fig. **54–59.** *Paramecium* (*Viridoparamecium*) *chlorelligerum* in the scanning electron microscope. **54, 55.** Ventral and dorsal overview, showing body shape variability and beautiful metachronal ciliary waves. The fragile caudal cilia are not preserved. **56, 59.** Deciliated specimens show the typical cortex structure of *Paramecium*. **57.** The caudal cilia are about thrice as long as the ordinary somatic cilia; both are heavily shrunken due to the preparation procedures. **58.** Oral area, showing the nonciliated postoral field (asterisk), containing, however, basal bodies (Fig. 46, 50, 52). AS, anterior (preoral) suture; CC, caudal cilia; OO, oral opening. Scale bars 5 μm (Fig. 56), 10 μm (Fig. 57, 58), 20 μm (Fig. 59), and 50 μm (54, 55).

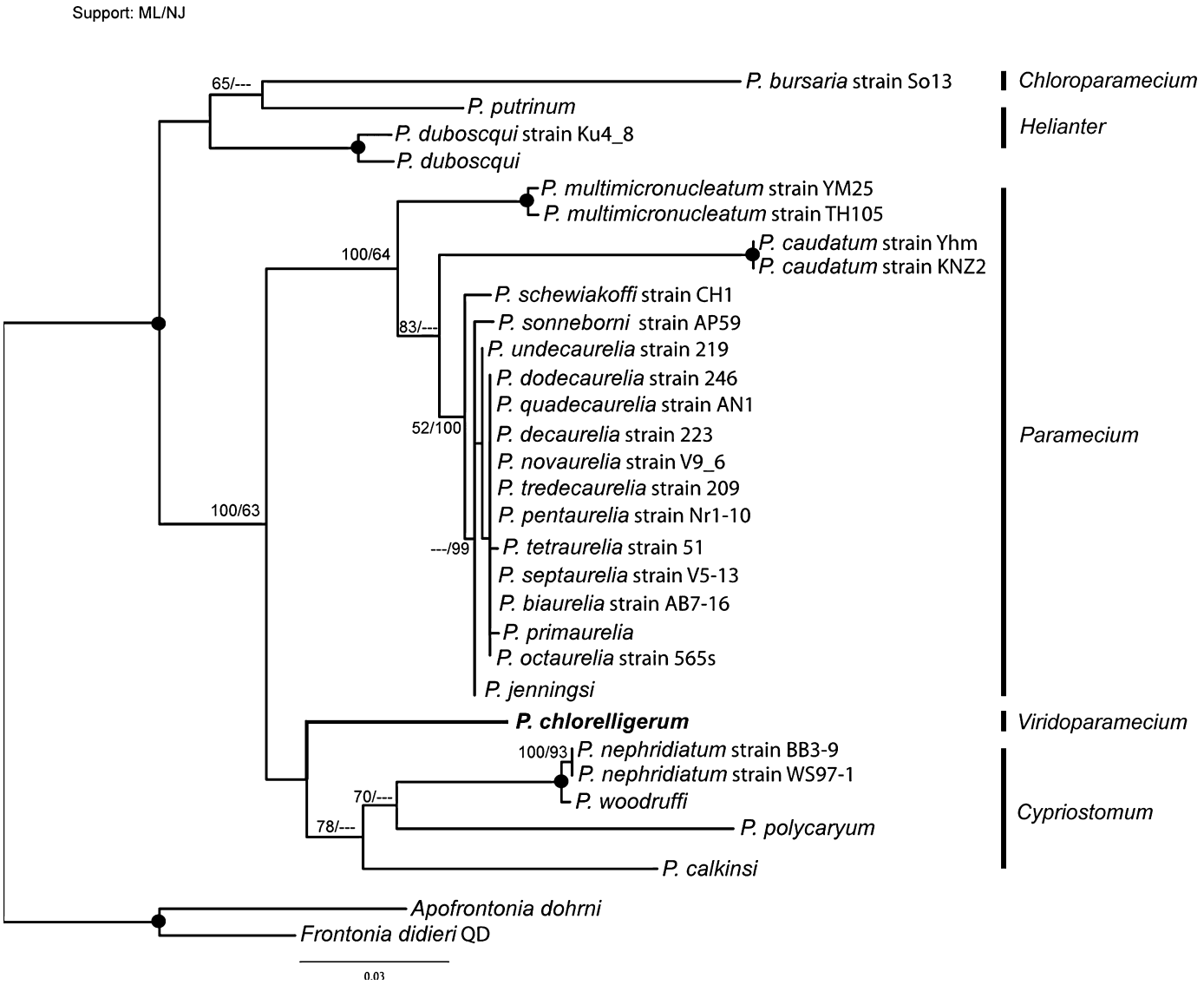

Fig. **60.** A maximum-likelihood (ML) tree showing the phylogenetic placement of *Paramecium (Viridoparamecium) chlorelligerum* (in bold) based on the 18S rRNA gene sequence. Bootstrap values above 50 for the ML (1,000 replicates) and neighbour-joining evolutionary distance (BioNJ, 1,000 replicates) analyses are given at the individual nodes. Large dots at nodes indicate full support from both tree construction methods. For details, see Methods section. Green (with symbiotic algae) species occur in two clades: *Paramecium bursaria* (green), *Paramecium putrinum, Paramecium duboscqui* and in *Paramecium chlorelligerum* (green), *Paramecium nephridiatum, Paramecium woodruffi*, *Paramecium polycaryum,* and *Paramecium calkinsi*.

extrusomes are about 7 μm long and produce a distinct fringe in the periphery of the cell. When exploded, the extrusomes are 30–40 μm long and show a strongly refractive, 2–3 μm long, needle-shaped tip (Fig. 3, 14, 22–34).

Cytoplasm and symbiotic algae. The cytoplasm is clear and colourless but the cells are green due to about 500 algal cells/specimen (Table 1 and Fig. 3, 13–16, 19, 25, 27, 28). The broadly ellipsoidal algal cells are 4.8–9.6 × 3.4–9.6 μm in size, on average 7.7 × 5.5 μm. The algae are surrounded by a perialgal vacuole and have two chromatophores, leaving blank one polar region. When dividing, each cell generates four offspring of much smaller size (Fig. 28–30, 44).

***Somatic ciliature* (Table 1 and Fig. 3–5, 13, 14, 17, 19, 43, 46, 50–59).** The cilia are about 10 μm long in vivo and arise from quadrangular (monokinetids) and hexagonal (dikinetids) kinetosomal territories. They produce beautiful metachronal waves and their basal bodies are associated with an ~ 10 μm long kinetodesmal fibre (Fig. 43, 54–56, 59). Furthermore, the basal bodies are accompanied by a parasomal sac at the right side of the monokinetids, while the dikinetids and their parasomal sac form minute triangles in the anterior half of the ventral side and the anterior fifth of the dorsal side (Fig. 3–5, 46, 50–55). In the right corner of the oral entrance is a patch of densely spaced monokinetids that are not ciliated (Fig. 4, 46, 50–52, 58). The ciliary pattern is as in congeners: there are a distinct preoral suture, which extends obliquely onto the dorsal side, and an indistinct posterior suture that contains the cytopyge (Fig. 3–5, 46, 50–55).

The special arrangement of the ciliary rows makes them difficult to count. Thus, we counted the rows in mid-body of the

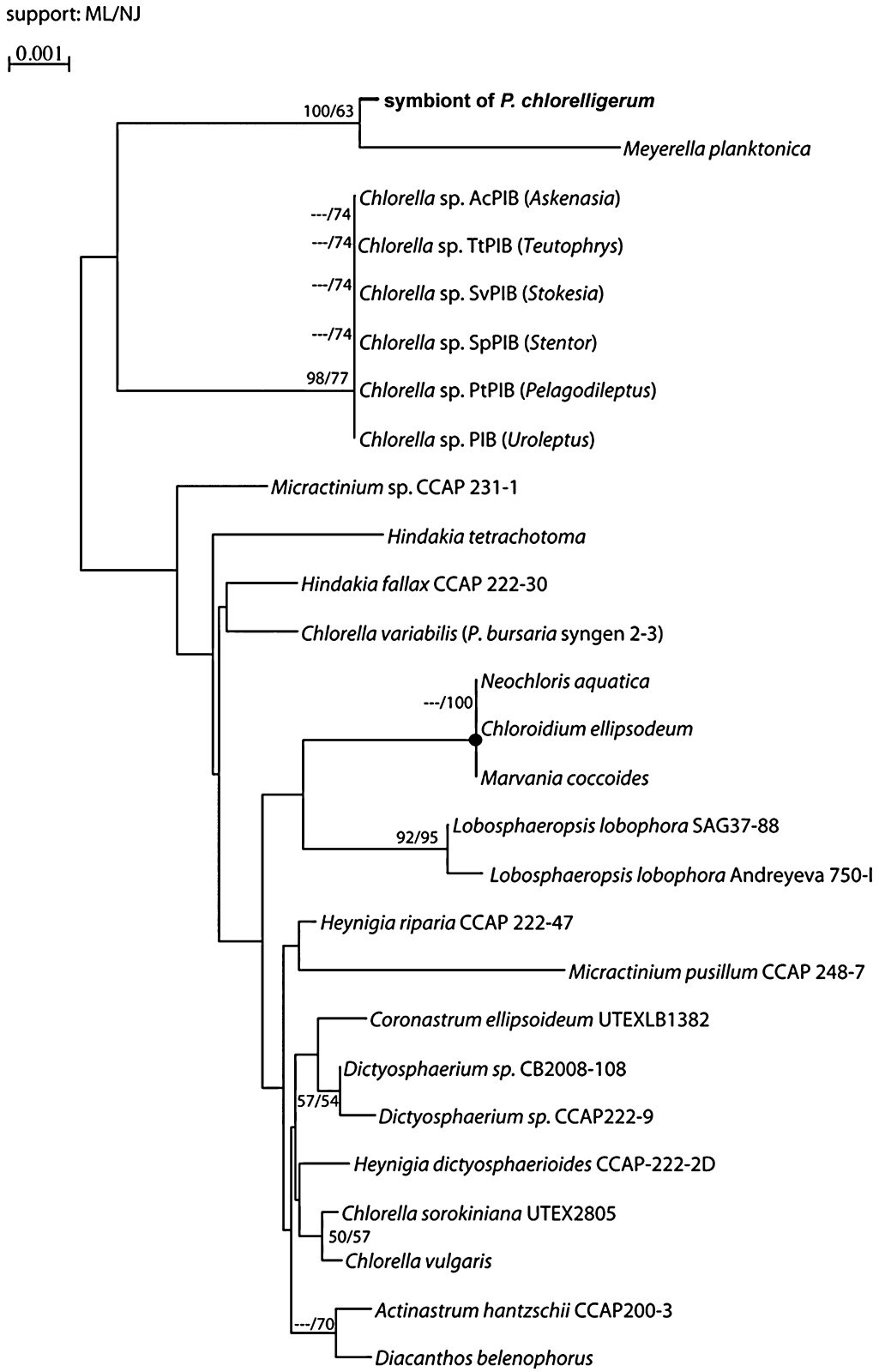

Fig. **61.** A maximum-likelihood tree showing the phylogenetic placement of the green algal symbiont (in bold) of *Paramecium (Viridoparamecium) chlorelligerum* based on the 18S rRNA gene sequence. Bootstrap values above 50 for the ML (1,000 replicates) and neighbour-joining evolutionary distance (BioNJ, 1,000 replicates) analyses are given at the individual nodes. The large dot indicates full support from both tree construction methods. For details, see Methods section.

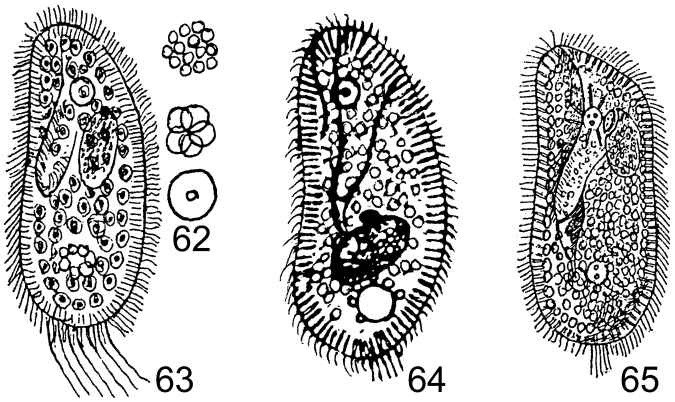

Fig. **62–65.** Literature illustrations of *Paramecium* species. **62, 63.** Contractile vacuole cycle and overview of *Paramecium chlorelligerum*, length 90 μm (after Kahl 1935). **64.** *Paramecium chlorelligerum*, length 88 μm (after Vuxanovici 1960). **65.** *Paramecium bursaria*, length 150 μm (after Kahl 1931).

Table **2.** Comparison of *Paramecium (Viridoparamecium) chlorelligerum* with *Paramecium (Chloroparamecium) bursaria*.

Characteristics	*Paramecium (Viridoparamecium) chlorelligerum*	*Paramecium (Chloroparamecium) bursaria*
With an ellipsoidal, rapidly swimming state	Yes	No
Average length of caudal cilia	29 μm	18 μm
Average size of micronucleus	5.7 × 2.4 μm	14 × 7 μm
Average size of symbiotic algae	7.7 × 6.2 μm	5.5 × 5.1 μm
Contractile vacuoles	With collecting vesicles	With collecting canals
Excretory pores/ contractile vacuole	1	2–3

dorsal side across an area of 20 μm (Table 1). These values were used to calculate the range (79–115 rows) and the average (98), assuming that the body is circular.

There are 10–12 caudal cilia, forming a transverse line on the posterior pole of the cell. The caudal cilia are 21–40 μm long, on average 29 μm, and difficult to preserve because the distal half is very fine and fragile (Table 1 and Fig. 3, 13, 14, 17, 19). They do not beat but can be spread, and when the cell swims, they form a train.

Oral ciliature. The pyriform oral entrance is in mid-body and has an average size of 13.1 × 4.5 μm in silver nitrate preparations (Table 1 and Fig. 3, 4, 24, 50, 52, 58). The oral ciliature is as in congeners (Fig. 6): there are a short paroral and three massive polykinetids or peniculi, each composed of four rows of narrowly spaced cilia. Proximally, the ciliary rows decrease in length, especially in the dorsal polykinetid (quadrulus), which becomes tailed and produces long pharyngeal fibres in the posterior half. In the anterior third of the quadrulus, the four ciliary rows are slightly spread but not disordered (Fig. 6).

Division and conjugation. During our studies, we saw more than 1,000 specimens but only two were dividing and one was conjugating (Fig. 26).

***Paramecium (Chloroparamecium) bursaria* (Ehrenberg 1831) Focke 1836 (Tables 1, 3 and Fig. 9, 10, 27, 34–39, 42, 45, 47, 48, 60, 65).** For comparison with *P.* (*V.*) *chlorelligerum*, we re-investigated the second green species, *P.* (*C.*) *bursaria*, with the same methods. The data are collected in Table 1 and the figures cited above. Thus, the description will be brief, emphasizing those features that are different.

The size and shape are as in *P.* (*V.*) *chlorelligerum* but the special "swimming shape" is absent (Table 1 and Fig. 13, 27). The macronucleus is as in *P.* (*V.*) *chlorelligerum*; the micronucleus belongs to the same "compact type" but is much larger (14 × 7 μm vs. 5.7 × 2.4 μm; Fig. 40, 42). The contractile vacuoles are markedly different (Fig. 28–33 vs. 34–39): with collecting canals in *P. chlorelligerum* and collecting vesicles in *P. bursaria* and several vs. one excretory pores/vacuole, respectively. The extrusomes and the cytoplasm are as in *P.* (*V.*) *chlorelligerum*. The symbiotic algae are distinctly different (Table 1 and Fig. 44, 45) in body size (i.e. 7.7 × 6.2 μm vs. 5.5 × 5.1 μm) and shape (i.e. a cup-shaped vs. two ellipsoidal chloroplasts) of the chromatophores. We conclude that the two algal species belong to different genera (see below).

The somatic ciliary pattern is inseparable from that of *P.* (*V.*) *chlorelligerum* (Table 1 and Fig. 46–48, 50). However, the caudal cilia are much shorter (i.e. 18 μm vs. 29 μm long on average), whereas the number of ciliary rows is slightly higher (i.e. 96–134 rows, $\bar{x}$ 117 vs. 79–115 rows, $\bar{x}$ 98; Table 1 and Fig. 17–19). The mouth entrance is as in *P.* (*V.*) *chlorelligerum* (Table 1). The oral ciliature was not studied.

***Paramecium* (*Cypriostomum*) *nephridiatum* Gelei 1925 (Fig. 49).** *Paramecium* (*C.*) *nephridiatum* is possibly rather closely related to *P.* (*V.*) *chlorelligerum*. This species has been carefully redescribed by Fokin et al. (1999b). Thus, we provide only a single figure (Fig. 49), showing that the ciliary pattern is quite similar to those of *P.* (*V.*) *chlorelligerum* (Fig. 46, 50, 52) and *P.* (*C.*) *bursaria* (Fig. 47, 48). However, the oral opening is not in mid-body but more posterior.

Molecular sequencing of *Paramecium* (*Viridoparamecium*) *chlorelligerum* (Fig. 60). According to the phylogenetic analyses of the 18S rRNA gene of *P.* (*V.*) *chlorelligerum*, this species represents a distinct evolutionary lineage within the genus *Paramecium* and does not fall within any other sequenced *Paramecium* clade. The position as sister branch to the *P. nephridiatum*/*P. woodruffi*/*P. calkinsi*/*P. polycaryum* clade is not supported by either tree construction method. The closest related sequence is that of *P. primaurelia* with 93.5% similarity.

Molecular sequencing of the symbiotic alga of *Paramecium* (*Viridoparamecium*) *chlorelligerum* (Fig. 61). The 18S rRNA gene sequence of the algal symbiont does neither branch with the *Chlorella* symbionts of *P.* (*C.*) *bursaria* or with *Chlorella* symbionts from a number of different ciliates. Instead, the *P. (V.) chlorelligerum* symbiont branches with *Meyerella planctonica*, with full statistical support from the ML analysis and an NJ distance bootstrap support of 63. The *P.* (*V.*) *chlorelligerum* symbiont shares 99.1% sequence similarity with *M. planctonica,* and thus most likely belongs to the same genus or even species.

DISCUSSION

Comparison with original description. Kahl (1935, p. 830; Fig. 62, 63) described *P.* (*V.*) *chlorelligerum* as follows (translated from German): "This green species, which is 80–100 μm in size, differs from *P. bursaria* by the more slender shape. According to the simple p. l. (we could not decipher this

Table **3.** Comparison of *Paramecium (Viridoparamecium) chlorelligerum* with clade congeners.

Characteristics[b]	*Paramecium (Viridoparamecium) chlorelligerum*	*Paramecium (Cypriostomum) calkinsi*[a]	*Paramecium (Cypriostomum) woodruffi*[a]	*Paramecium (Cypriostomum) nephridiatum*[a]	*Paramecium (Cypriostomum) polycaryum*[a]
Body, length (μm; CHL)	106–120 (112)[c]	60–160 (120)	120–210 (170)	90–170 (130)	70–130 (85)
Body, width (μm; CHL)	41–60 (51)	20–80 (40)	40–80 (55)	30–60 (41)	35–60 (40)
Body width: length, ratio (CHL)	0.46	0.33	0.32	0.29	0.47
Swimming shape (IV)	Present	Absent	Absent	Absent	Absent
Symbiotic algae (IV)	Present	Absent	Absent	Absent	Absent
Micronuclei, type (P)	Compact	Endosomal	Endosomal	Endosomal	Vesicular
Micronuclei, length (μm; P)	4.1–6.9 (5.7)[d]	2–4 (3)	3–5 (4)	1.5–4 (3)	1.4–8 (1.6)
Micronuclei, number (P)	1 (1)	1–5 (2)	0–10 (4)	1–7 (3)	0–8 (4)
Micronuclei, position (P)	Near macronucleus	Near macronucleus	Anteriorly	Anteriorly	Near macronucleus
CV with vesicles or canals (IV)	Vesicles	Canals	Canals	Canals	Canals
Excretory pores, number/vacuole (CHL)	1 (1)	1 (1)	1 (1)	1–5 (2)	1–2
Environment	F	F, B, S	F, B, S	F, B, S	F

[a]From Fokin and Chivilev (1999).
[b]Based on 20–25 specimens each.
[c]Values in brackets are arithmetic means.
[d]In vivo.
B = brackish; CHL = Chatton–Lwoff silver nitrate impregnation; F = freshwater; IV = in vivo; P = preparation; S = sea water.

abbreviation), *P. chlorelligerum* appears closely related to *P. trichium* but the contractile vacuoles are formed by small vesicles (Fig. 62). The oval macronucleus is accompanied by a globular micronucleus 3–4 μm across. I know this species only from the mud of a mire puddle, where it is sometimes abundant." Kahl (1935) supplemented this short and rather incomplete description by one of his excellent line drawings, showing two further important features: the long caudal cilia and a single excretory pore for each contractile vacuole. All these features match our population, suggesting that the identification is correct.

Distinguishing *Paramecium* (*Viridoparamecium*) *chlorelligerum* from *Paramecium* (*Chloroparamecium*) *bursaria* (Table 2). These species are not easily distinguished because they have a similar size, shape, and colour. In vivo identification needs at least the inspection of the contractile vacuoles: with small collecting vesicles and a single excretory pore for each contractile vacuole in *P.* (*V.*) *chlorelligerum* vs. collecting canals and 2–3 excretory pores for each contractile vacuole in *P.* (*C.*) *bursaria*. In silver preparations, the excretory pores (1 vs. 2–3) and the size of the micronuclei (~ 6 × 3 μm vs. 14 × 7 μm) should suffice.

In the swimming state, *P.* (*V.*) *chlorelligerum* highly resembles some green prostomatids, such as *Holophrya ovum* and *Pelagothrix* spp. Thus, it is easily misidentified at superficial inspection of samples.

The features listed in Table 2 need some discussion as their significance must be interpreted with the appropriate level of background knowledge about diversity within the genus *Paramecium*. When not explicitly stated otherwise, we refer to the reviews of Fokin et al. (2004), Kahl (1931), Nyberg (1988), Wenrich (1928), and Wichterman (1986).

(i) A special swimming shape, as present in *P.* (*V.*) *chlorelligerum*, has not been reported from any other *Paramecium* species and should thus be considered a specific character of *P.* (*V.*) *chlorelligerum*. Interestingly, Kahl (1935) did not mention this distinctive feature. Possibly, he confused the rapidly swimming, cylindroidal to ellipsoidal specimens with green prostomatids, such as *Holophrya* spp. and *Pelagothrix* spp., as we did for some time.

(ii) Kahl (1935) did not mention but illustrated the long caudal cilia of *P.* (*V.*) *chlorelligerum*. The length of the caudal cilia has never been used as a species character in *Paramecium*, possibly because it is difficult to measure or similar in most species. Indeed, the caudal cilia of the large *P. caudatum* have a similar length (~ 16 μm, Machemer-Röhnisch and Machemer 1984; Wichterman 1986) as those of the small *P.* (*C.*) *bursaria* (18 μm, Table 2). Thus, the 30-μm long caudal cilia of *P.* (*V.*) *chlorelligerum* are an exception and a reliable feature of the species.

(iii) The size of the micronucleus is conspicuously different in *P.* (*V.*) *chlorelligerum* and *P.* (*C.*) *bursaria* (Table 2). Indeed, this feature is now widely accepted as an important species character in *Paramecium* (Fokin 1997). Our data from *P.* (*C.*) *bursaria* match well those of Fokin (1997), who found size and shape highly variable in five unimicronucleate and one bimicronucleate stock; however, five of the six stocks fall into the range of our data, while the micronucleus of stock Br80-6 is highly similar to that of *P.* (*V.*) *chlorelligerum*, suggesting that it may have been that species.

(iv) The symbiotic algae of *P.* (*V.*) *chlorelligerum* and *P.* (*C.*) *bursaria* have different shape (i.e. broadly ellipsoidal vs. almost globular) and size (Table 2). The molecular data show that they belong to two genera: *Meyerella* and *Chlorella*. We conclude that algal symbiosis developed independently in these two species. In *P.* (*C.*) *bursaria*, symbiosis evolved convergently with at least four different algae (Hoshina and Imamura 2008). Thus, the symbiotic algae are possibly of little value

for distinguishing *Paramecium* species. Thus far, only free-living *Meyerella* populations have been reported and to the best of our knowledge, no record exists from Europe (Fawley et al. 2005).

(v) There are three types of contractile vacuoles in *Paramecium* (Fokin 1986, 2010/11): with collecting canals (e.g. *P.* (*C.*) *bursaria*), with collecting vesicles (e.g. *P.* (*V.*) *chlorelligerum*), and with a long tube between vacuole and excretory pore (e.g. *P. trichium*). As far as we know, nobody has ever described any variability in the vacuole type, while the number of collecting canals is rather variable (Fokin and Chivilev 1999). Thus, the contractile vacuole type is a reliable species feature.

(vi) The number of excretory pores/vacuole is highly variable in various species (Fokin and Chivilev 1999; Fokin et al. 1999a, b; Günther 2006). However, the average number is fairly constant and thus a useful species feature (Fokin et al. 1999b). Of over 40 *P.* (*V.*) *chlorelligerum* specimens analysed, all have one excretory pore/vacuole, while *P.* (*C.*) *bursaria* usually has two pores/vacuole.

***Viridoparamecium*, a new subgenus of *Paramecium*.** *Paramecium* (*V.*) *chlorelligerum* attaches to the *P.* (*Cypriostomum*) *nephridiatum* clade but with low bootstrap support. However, it is unlikely that it will ever form a clade with *P.* (*C.*) *bursaria*. When *P.* (*V.*) *chlorelligerum* is compared with members of the *P.* (*C.*) *nephridiatum* clade, the following unique features can be seen (Table 3): *P.* (*V.*) *chlorelligerum* has a special swimming shape; symbiotic algae; and a single, compact micronucleus with an achromatic cap. These differences suggest classification of *P. chlorelligerum* in a distinct subgenus, *Viridoparamecium*. Actually, the situation is similar to that of *P. bursaria*, for which Fokin et al. (2004) established the subgenus *Chloroparamecium*.

Is *Paramecium* (*Viridoparamecium*) *chlorelligerum* a rare species? Compared with *P.* (*C.*) *bursaria*, *P.* (*V.*) *chlorelligerum* is likely rare because (i) we found only one report in the literature (Vuxanovici 1960) and (ii) rather many *P.* (*C.*) *bursaria* populations have been identified with molecular methods and did not provide any indication of a second green *Paramecium* species. Vuxanovici (1960) found many specimens of *P.* (*V.*) *chlorelligerum* in the clear water of Lake Herăstrău, in the surroundings of the town of Bucharest, Rumania. He described the caudal cilia as 8–10 μm long, very likely because he could not see their real length, especially the very fine distal half, with the simple microscope he used.

However, *P.* (*V.*) *chlorelligerum* is possibly not as rare as it appears. First, the mire environments that both Kahl (1935) and we investigated and in which we found *P.* (*V.*) *chlorelligerum* are little studied. Second, *P.* (*V.*) *chlorelligerum* might have been sometimes confused with *P.* (*C.*) *bursaria* or green prostomateans due to the ellipsoidal swimming shape (see above).

TAXONOMIC SUMMARY

Class Oligohymenophorea de Puytorac et al. 1974
Order Peniculida Fauré-Fremiet in Corliss 1956
Family Parameciidae Dujardin 1841
Genus *Paramecium* O. F. Müller 1773
Subgenus *Viridoparamecium* nov. subgen.

Diagnosis. A green (by symbiotic *Meyerella* sp.) *Paramecium*, producing a distinct clade, different from that of *P.* (*Chloroparamecium*) *bursaria* with the 18S rRNA gene.

Type species. *Paramecium chlorelligerum* Kahl 1935.

Etymology. Composite of the Latin adjective *viridis* (green) and the generic name *Paramecium* (slipper-shaped), meaning a green *Paramecium*.

Remarks. The suprageneric classification follows Lynn (2008). Neotypification of *P.* (*V.*) *chlorelligerum* is not necessary because the species can be reliably identified with Kahl's description and figures.

Species *Paramecium* (*Viridoparamecium*) *chlorelligerum* Kahl 1935

Improved diagnosis. Size in vivo 80–140 × 37–61 μm, on average 116 × 48 μm. With two shapes: resting specimens ellipsoidal to elongate ellipsoidal with concave preoral area and slow movement; turn to cylindroidal, very rapidly swimming cells when disturbed. Micronucleus of compact type, in vivo about 6 × 3 μm in size. Two contractile vacuoles each with collecting vesicles and a single excretory pore. About 98 ciliary rows. Caudal cilia 29 μm long on average. Oral entrance in mid-body.

Type locality. Mud of a clear moorland pond in the surroundings of the town of Hamburg (53°30′N/10°E), Germany, where Kahl (1935) lived and worked.

Type material. No original type material is available. Thus, we deposited five microscope voucher slides each with silver nitrate (Chatton–Lwoff method as described in Foissner 1991) and protargol-impregnated (Wilbert's method as described in Foissner 1991) environmental specimens of *P.* (*V.*) *chlorelligerum* in the Biologiezentrum of the Oberösterreichische Landesmuseum in Linz (LI), reg. no. 2012/2–2012/11. In addition, four and two voucher slides, respectively, of silver nitrate-impregnated environmental specimens of *P.* (*C.*) *bursaria* from the same habitat and cultivated specimens of *P.* (*C.*) *nephridiatum* from Bavaria (Germany) have been deposited in the same repository, reg. no. 2012/12–2012/17. Relevant specimens have been marked with black ink circles on the coverslip.

Remarks. We did not include the oral ciliary pattern in the diagnosis because it is very likely highly similar to that of other small *Paramecium* species (Dragesco and Dragesco-Kernéis 1986). Kahl (1935) did not specify the type locality, but it is certainly in the Hamburg area. Possibly, the type locality has been lost because the Hamburg moorland, where Kahl (1935) discovered many new species, became densely populated by man after World War II (Wenzel, F., pers. commun.).

ACKNOWLEDGMENTS

This study was supported by the Austrian Science Fund (FWF, projects 20360-B17 and 22846-B17) and the German Science Fund (DFG, project STO 414/3-2). The technical assistance of Mag. Barbara Harl, Johannes Rattey MSc, Robert Schörghofer, Hans Werner Breiner, and Andreas Zankl is greatly acknowledged.

LITERATURE CITED

Castresana, J. 2000. Selection of conserved blocks from multiple alignments for their use in phylogenetic analysis. *Mol. Biol. Evol.*, **17**:540–552.

Corliss, J. O. 1956. On the evolution and systematics of ciliated protozoa. *Syst. Zool.*, **5**:68–91, 121–140.

Dragesco, J. & Dragesco-Kernéis, A. 1986. Ciliés libres de l'Afrique intertropicale. Introduction a la connaissance et a l'étude des ciliés. *Faune tropicale (Éditions de l'Orstom, Paris)*, **26**:1–559.

Dujardin, F. 1841. Histoire naturelle des zoophytes. Infusoires. Suites à Buffon, Paris. p. 684.

Edgar, R. C. 2004. MUSCLE: multiple sequence alignment with high accuracy and high throughput. *Nucleic Acids Res*., **32**:1792–1797.
Ehrenberg, C. G. 1831. Über die Entwickelung und Lebensdauer der Infusionsthiere; nebst ferneren Beiträgen zu einer Vergleichung ihrer organischen Systeme. *Abh. preuss. Akad. Wiss., Phys.- math. Kl*., **1831**:1–154.
Fawley, M. W., Fawley, K. P. & Owen, H. A. 2005. Diversity and ecology of small coccoid green algae from Lake Itasca, Minnesota, USA, including *Meyerella planktonica*, gen. et sp. nov. *Phycologia*, **44**:35–48.
Focke, G. W. 1836. Über einige Organisationsverhältnisse bei polygastrischen Infusorien und Räderthieren. *Isis*, **10**:785–787.
Foissner, W. 1991. Basic light and scanning electron microscopic methods for taxonomic studies of ciliated protozoa. *Europ. J. Protistol*., **27**:313–330.
Foissner, W. 2003. Deciliation of ciliated protozoa for scanning electron microscopy: a fast, simple method using tensides. (Abstr.) 4th European Congress of Protistology and 10th European Conference on Ciliate Biology. Collection of Abstracts, San Benedetto, Italy. p. 133.
Fokin, S. I. 1986. Morphology of the contractile vacuoles in ciliated protozoa of the genus *Paramecium* (Hymenostomatida, Peniculina) as a species-specific character. *Zool. Zh*., **65**:5–15. (in Russian with English summary)
Fokin, S. I. 1997. Morphological diversity of the micronuclei in *Paramecium*. *Arch. Protistenk*., **148**:375–387.
Fokin, S. I. 2010/11. *Paramecium* genus: biodiversity, some morphological features and the key to the main morphospecies discrimination. *Protistology*, **6**:227–235.
Fokin, S. I. & Chivilev, S. M. 1999. Brackish water *Paramecium* species and *Paramecium polycaryum*. Morphometrical analysis and some biological peculiarities. *Acta Protozool*., **38**:105–117.
Fokin, S. I., Schweikert, M. & Fujishima, M. 2005. Recovery of the ciliate *Paramecium multimicronucleatum* following bacterial infection with *Holospora obtusa*. *Europ. J. Protistol*., **41**:129–138.
Fokin, S. I., Stoeck, T. & Schmidt, H. J. 1999a. *Paramecium duboscqui* Chatton, Brachon, 1933. Distribution, ecology and taxonomy. *Europ. J. Protistol*., **35**:161–167.
Fokin, S. I., Stoeck, T. & Schmidt, H. J. 1999b. Rediscovery of *Paramecium nephridiatum* Gelei, 1925 and its characteristics. *J. Eukaryot. Microbiol*., **46**:416–426.
Fokin, S. I., Przyboś, E., Chivilev, S. M., Beier, C. L., Horn, M., Skotarczak, B., Wodecka, B. & Fujishima, M. 2004. Morphological and molecular investigations of *Paramecium schewiakoffi* sp. nov. (Ciliophora, Oligohymenophorea) and current status of distribution and taxonomy of Paramecium spp. *Europ. J. Protistol*., **40**:225–243.
Galtier, N., Gouy, M. & Gautier, C. 1996. SEAVIEW and PHYLO_-WIN: two graphic tools for sequence alignment and molecular phylogeny. *Comput. Appl. Biosci*., **12**:543–548.
Gelei, J. 1925. Uj *Paramecium* szeged kornyekerol. *Paramecium nephridiatum nov. spec. Zool. Mitt*., **22**:121–162. (in Hungarian with German summary)
Görtz, H.-D. ed. 1988. *Paramecium*. Springer, Berlin. 444 p.
Günther, G. 2006. Variabilität der Expulsionsporenanzahl bei *Paramecium bursaria*. *Mikrokosmos*, **95**:265–269.
Hoshina, R. & Imamura, N. 2008. Multiple origins of the symbioses in *Paramecium bursaria*. *Protist*, **159**:53–63.
Hoshina, R., Hayashi, S. & Imamura, N. 2006. Intraspecific genetic divergence of *Paramecium bursaria* and re-construction of the Paramecian phylogenetic tree. *Acta Protozool*., **45**:377–386.
Jankowski, A. W. 1972. Cytogenetics of *Paramecium putrinum* C. et L., 1858. *Acta Protozool*., **10**:285–394.
Kahl, A. 1931. Urtiere oder Protozoa I: Wimpertiere oder Ciliata (Infusoria) 2. Holotricha außer den im 1. Teil behandelten Prostomata. *Tierwelt Dtl*., **21**:181–398.
Kahl, A. 1935. Urtiere oder Protozoa I: Wimpertiere oder Ciliata (Infusoria) 4. Peritricha und Chonotricha. *Tierwelt Dtl*., **30**:651–886.
Kreutz, M. & Foissner, W. 2006. The *Sphagnum* ponds of Simmelried in Germany: a biodiversity hot-spot for microscopic organisms. *Protozool. Monogr*., **3**:1–267.
Lopez-Garcia, P., Rodriguez-Valera, F., Pedros-Alio, C. & Moreira, D. 2001. Unexpected diversity of small eukaryotes in deep-sea Antarctic plankton. *Nature*, **409**:603–607.
Lynn, D. H. 2008. The Ciliated Protozoa. Characterization, Classification, and Guide to the Literature, 3rd ed. Springer, Dordrecht. i–xxxiii + 605 p.
Machemer-Röhnisch, S. & Machemer, H. 1984. Receptor current following controlled stimulation of immobile tail cilia in *Paramecium caudatum*. *J. Comp. Physiol. A*., **154**:263–271.
Medlin, L., Elwood, H. J., Stickel, S. & Sogin, M. L. 1988. The characterization of enzymatically amplified eukaryotic 16S-like rRNA-coding regions. *Gene*, **71**:491–499.
Müller, O. F. 1773. Vermium Terrestrium et Fluviatilium, seu Animalium Infusorium, Helminthicorum et Testaceorum, non Marinorum, Succincta Historia. Heineck & Faber, Havniae & Lipsiae. 135 p.
Nakahara, M., Tsubota, H., Handa, S., Watanabe, S. & Deguchi, H. 2004. Molecular phylogeny of *Chlorella*-like symbiotic algae in *Paramecium bursaria* based on 18S rRNA gene sequences. *Hikobia*, **14**:129–142.
Nyberg, D. 1988. The species concept and breeding systems. *In*: Görtz, H.-D. (ed.), *Paramecium*. Springer, Berlin. p. 41–58.
Plattner, H. 2002. My favorite cell–*Paramecium*. *BioEssays*, **24**: 649–658.
Plattner, H. & Kissmehl, R. 2003. Molecular aspects of membrane trafficking in *Paramecium*. *Int. Rev. Cytol*., **232**:185–216.
Przyboś, E. & Fokin, S. 2000. Data on the occurrence of species of the *Paramecium aurelia* complex world-wide. *Protistology*, **1**: 179–184.
Przyboś, E., Maciejewska, A. & Skotarczak, B. 2006. Relationships of species of the *Paramecium aurelia* complex (Protozoa, Ph. Ciliophora, Cl. Oligohymenophorea) based on sequences of the histone H4 gene fragment. *Folia Biol. (Krakow)*, **54**:37–42.
de Puytorac, P., Batisse, A., Bohatier, J., Corliss, J. O., Deroux, G., Didier, P., Dragesco, J., Fryd-Versavel, G., Grain, J., Grolière, C., Hovasse, R., Iftode, F., Laval, M., Roque, M., Savoie, A. & Tuffrau, M. 1974. Proposition d'une classification du phylum Ciliophora Doflein, 1901 (réunion de systématique, Clermont-Ferrand). *C. r. hebd. Séanc. Acad. Sci., Paris*, **278**:2799–2802.
Sonneborn, T. M. 1975. The *Paramecium aurelia* complex of fourteen sibling species. *Trans. Am. Microsc. Soc*., **94**:155–178.
Stamatakis, A., Hoover, P. & Rougemont, J. 2008. A fast bootstrap algorithm for the RAxML web-servers. *Syst. Biol*., **57**:758–771.
Strüder-Kypke, M. C., Wright, A. -D. G., Fokin, S. I. & Lynn, D. H. 2000. Phylogenetic relationships of the genus *Paramecium* inferred from small subunit rRNA gene sequences. *Mol. Phylogenet. Evol*., **14**:122–130.
Vuxanovici, A. 1960. Noi contributii la studiul ciliatelor dulcicole din Republica Populara Romîna (nota 1). *Studii. Cerc. Biol. (Biol. Anim.)*, **12**:353–381. (in Rumanian with Russian and French summaries)
Wenrich, D. H. 1928. Eight well-defined species of *Paramecium* (Protozoa, Ciliata). *Biol. Bull*., **56**:390–401.
Wichterman, R. 1986. The Biology of *Paramecium*, 2nd ed. Plenum Press, New York, London. 599 p.
Wilbert, N. 1975. Eine verbesserte Technik der Protargolimprägnation für Ciliaten. *Mikrokosmos*, **1975**:171–179.

SUPPORTING INFORMATION

Additional Supporting Information may be found in the online version of this article:

Video S1. Movement of *Paramecium chlorelligerum*.

Please note: Wiley-Blackwell is not responsible for the content or functionality of any Supporting Information supplied by the authors. Any queries (other than missing material) should be directed to the corresponding author for the article.

Received: 03/07/12, 05/08/12; accepted: 05/11/12